2. TOKAMAK ISTTOK

C.A.F. Varandas and J.A.C. Cabral (Heads), M.P. Alonso, P. Amorim, H. Fernandes, H. Figueiredo, R. Gomes, T. Madeira, I. Nedzelkij, J. Pereira, R. Pinheiro, J.M. Pires, V. Plyusnin, C. Silva, A. Soares and E. Sokolova

2.1. INTRODUCTION

The tokamak ISTTOK was in operation during about 20 weeks in 2000, due to several problems with the slow control system.

The research and development (R&D) activities have been mainly centred in the following topics:

- Discharge production systems
- Diagnostics
- Plasma physics studies

2.2. Discharge production systems

The main tasks carried out in this area have been:

- Repair of the commercial vacuum controller unit of the slow control system.
- Repair of two turbo-molecular pumps of the main vacuum system.
- Design, construction and implementation of a new slow control system. An alternative vacuum control system is already in operation.

2.3. Diagnostics

2.3.1. Introduction

The main tasks performed in this area have been:

- Implementation of a new set of three emissive Langmuir probes for the determination of the edge plasma potential profile[1]. The probes are mounted on the same poloidal plane. Their lengths have been adjusted so that their tips are on different minor radii in the plasma scrape-off layer.
- Improvement of the ion gun of the heavy ion beam diagnostic in order to increase the beam current[2].
- Installation of a movable electrode for plasma biasing on ISTTOK
- Implementation of a second optical fibre on the Thomson scattering diagnostic aiming at allowing the measurement of the electron temperature simultaneously at two plasma points
- Absolute calibration of the Thomson scattering diagnostic for measurements of the electron temperature

2.3.2. New ion gun of the heavy ion beam diagnostic

The initial injection system of the heavy ion beam diagnostic (HIBD) provides a 2 mm diameter and 3.6 mrad divergence beam of Cs^+ ions, after extraction from a plasma ion source and acceleration up to 20 keV, by a gap lens and diameter definition by a set of defining apertures. However, the intensity of the beam is strongly reduced to 1.5 μA, therefore complicating the HIBD measurements of the plasma parameters, especially those of the plasma electric potential by the time-of-flight (TOF) method.

A new injection system, which is able to work with both a solid-state thermo-ionic source and a mono-cusp plasma ion source, has been designed and built in a 100 kV multi-sectional acceleration tube (Fig. 2.1). A 135^o cone-shaped Pierce electrode, with 2 mm aperture, and a 120^o cone-shaped extraction electrode, with 14 mm aperture constitute the extraction gap. The electrodes of the following acceleration tube are split in three groups. The electrodes inside the first (lens) and the second (drift space) groups are short-circuited. The third group of electrodes arranges the final acceleration gap.

Optimisation experiments with the new injector have been made by namely the study of the dependences of the beam intensity at the output of the injection system with the effective extraction potential, for solid-state thermo-ionic and mono-cusp plasma ion sources. The beam dimensions in the focus point, standing 1.3 m from the injector, remain just the same as the initial injection system, but the intensity increases 7.3 times with a solid-state ion source and 26 times with a plasma source. The beam

[1] Work carried out in collaboration with the University of Innsbruck of the Association EURATOM/OAW.
[2] Work performed in collaboration with IPP-Kharkov.

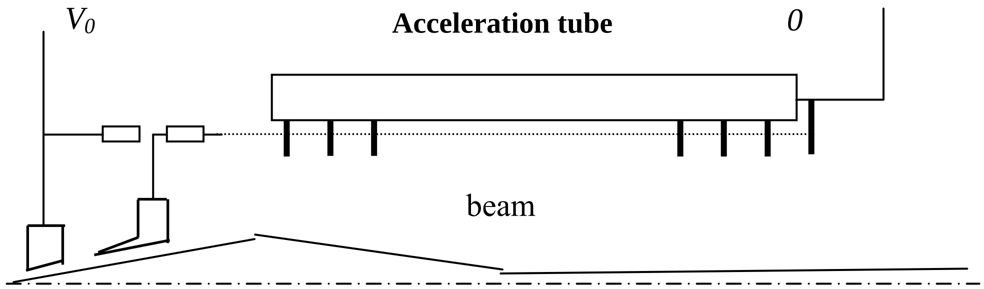

Fig. 2.1 – Schematic drawing of the new ion gun

divergence is respectively 2.5 times lower and 4 times higher. The observed difference in the output currents with solid-state and plasma ion sources is the result of a difference of the shapes of the respective emission surfaces, that are respectively flat and convex. The experimental results are well matched to the Child-Langmuir law applied to the extraction gap (solid curves in Fig. 2.2).

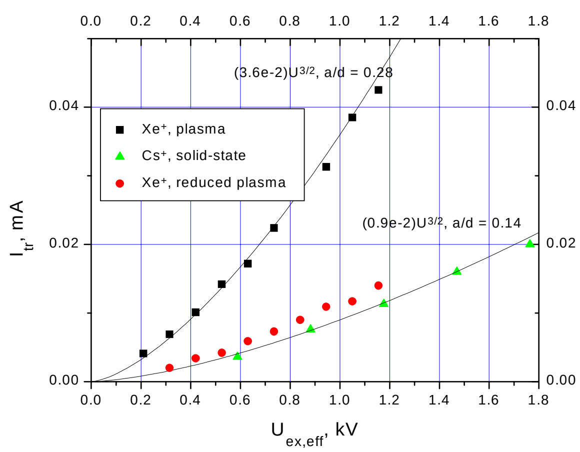

Fig. 2.2 – Results of the optimisation experiments for a solid-state thermo-ionic source (triangles) and a mono-cusp plasma source (squares).

2.3.3. Movable electrode for plasma biasing on ISTTOK

A movable electrode has been developed to modify the radial electric field at the plasma edge and to complement the limiter biasing experiments (Fig. 2.3).

The electrode is held by a stainless steel body, which controls its movement, which is achieved by sliding the system over two guiding rods. The overall stroke length of the bellow is 106 mm.

The mushroom shaped electrode head is made of 2-D carbon composite, screwed to a stainless steel shaft that is protected by boron nitride as an insulating material to be exposed to the plasma. The choice of the carbon composite, as conductive material to be exposed to the plasma, has been done to have a low Z and high thermal conductivity material. The surfaces have been smoothed and sharp angles have been avoided to decrease the power density on the electrode.

2.4. Plasma physics studies

2.4.1. Introduction

The main activities carried out in this area have been:

- Study of the runaway generation and of the disruptive instability
- Analysis of the plasma stability modifications produced by an external helical current established between the two tokamak localised limiters.
- Study of the modifications in both plasma confinement and stability arising from a limiter biasing process with an alternating voltage.
- Determination of the edge plasma potential profile with the new set of emissive Langmuir probes.
- Plasma potential measurements by the HIBD with a time-of-flight method.

2.4.2. Runaway generation and the disruptive instability

Discharges with a significant amount of runaway electrons are reproducibly obtained in the experiments carried out on ISTTOK. A specific

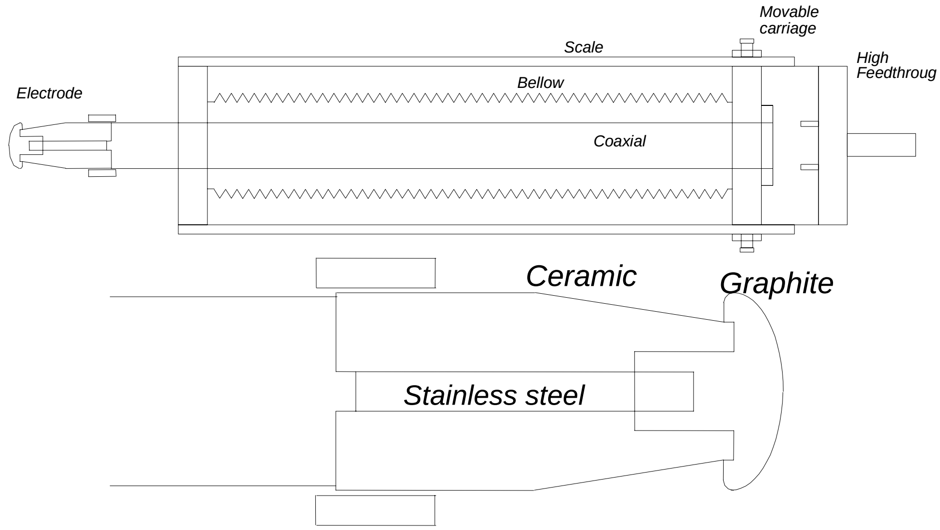

Fig. 2.3 - Schematic of the electrode system and an enlarged view of the head.

feature of the experiments is that they are characterized by the high current drift velocity values ($u_{drift} \sim v_{Te}$) due to the high longitudinal electric field ($E_0 \geq 1$V/m) at low plasma density. In this case the runaway process is caused by the primary (Dreicer) mechanism. Discharges enter into runaway regimes at low critical values of the electron velocity

$$v_{cr}=v_{Te}\,(E_{cr}/E_0)^{1/2},\; E_0<E_{cr}, \qquad (2.1)$$

where

$$E_{cr}=e^3 \ln\Lambda n_e Z_{eff}/4\pi\varepsilon^2 T_e \qquad (2.2)$$

is the Dreicer field, *e* the elementary charge, Z_{eff} the effective ion charge, and l Λ is the Coulomb logarithm.

The runaway-related events, including typical relaxation phenomena as a result of the runaway instability, have been observed in discharges with relatively high current density values $<j_{pl}> \cong 0.2$-0.5 MA/m^2 in the plasma density range 1 to $5\times10^{18} m^{-3}$.

The Dreicer mechanism of the runaway generation is very sensitive to the electron temperature. This parameter was calculated from the measured loop voltage and plasma current using the usual formula of the plasma resistivity given by Spitzer and Härm and taking into account the resistivity correction factor in impure plasmas. Spectroscopic measurements indicate the presence of impurities, but it was not possible to evaluate accurately the values of Z_{eff}. Therefore, the evaluation of the runaway regimes from the experimental data was started using the results of the preliminary numerical modelling. In this modelling the evolution of the discharge parameters was simulated including the effect of the primary runaway generation in zero-dimensional approximation. The 0-D model code includes the equations of energy balance for electrons, ions and atoms as well as particle balance equations with typical confinement times about 0.1-0.4 ms. This set of equations was completed by the equations of the electric circuit for capacitor battery driven discharge in equivalent ‘perfect transformer’ scheme and by an equation of evolution of runaway electron density for calculation of the runaway current (I_r) in the continuous creation model.

The power-energy balance study enabled to estimate reasonable limits of the electron temperature and effective ion charge, being the other macroscopic parameters chosen close to the experimental ones. In this case the modeling yields the runaway current values I_r ~1-5 kA, which are adequately fitted to the ranges of plasma parameters variation during runaway events. Taking the obtained results as an initial condition and matching them to the experimental data the values of runaway current were calculated. These calculations, obtained from the experimental data have shown that the number of electrons diffused into the runaway regime is high enough to carry out a significant fraction of the total plasma current (up to 20%) (Fig. 2.4).

Slightly lower plasma density in #8570 in comparison to #8568 resulted in significantly higher

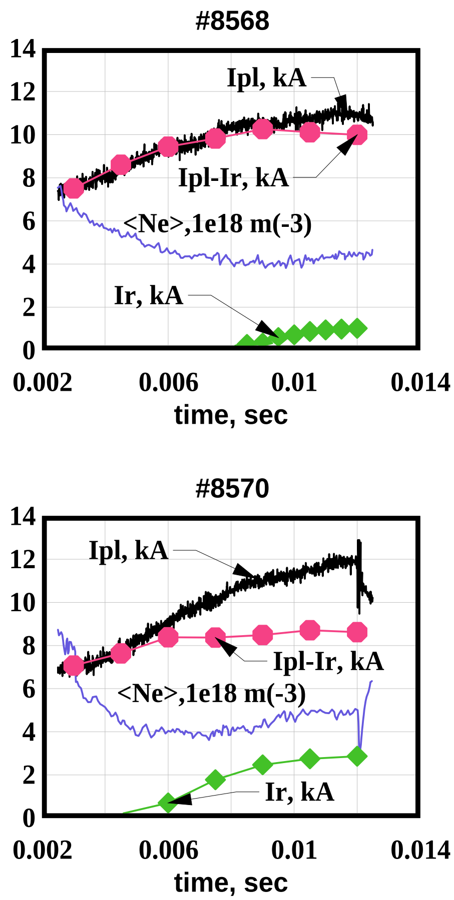

Fig. 2.4 - The evolution of the runaway current in shots #8568 and #8570.

runaway fraction (I_r) in the first shot. Such an uncontrolled increase of the runaway fraction as well as of the total plasma current led to the temporary loss of the MHD stability of the plasma column ($q(a) \cong 3.2$) and to minor disruptions.

The instability driven by runaway electrons was observed in the experiments. It occurs at the condition

$$\omega_{ce}/\omega_{pe} \geq 1 \qquad (2.3)$$

due to the anomalous Doppler effect. This instability is accompanied by the excitation of magnetized Langmuir oscillations. The scattering of the electrons on these oscillations leads to the isotropisation of the runaway beam in the velocity space. If the density of accelerated electrons is sufficiently high, the isotropisation of their distribution function can be considered as an increase of the plasma effective electron temperature, a decrease of the plasma resistance and the appearance of negative loop voltage spikes (Fig. 2.5). This effect was observed in the experiments. The positive loop voltage spikes during the instability events were also observed. This phenomenon is associated with changes in the effective plasma resistance due to the loss of momentum by the accelerated electrons during diversion. Positive loop voltage spikes themselves are evidence for the fact that the effect of the runaway electron retardation becomes noticeable when the runaway electron current is a significant fraction of the total plasma current. According to the theory of runaway instability, the above described phenomena develops if the criterion concerning the relation between the beam velocity and the electron runaway critical velocity is satisfied:

$$v_{beam} \geq 3 v_{cr} \, (\omega_{ce}/\omega_{pe})^{3/2} \qquad (2.4)$$

Since

$$v_{cr} = v_{Te} \, (E_{cr}/E_0)^{1/2} \qquad (2.5)$$

a simple evaluation at the given experimental parameters ($\langle n_e \rangle$, V_{loop}) and $\langle T_e \rangle$~40-60 eV shows that $v_{beam}/v_{Te} \geq 10$ and, due to the low value of the electron temperature, the instability threshold can easily be achieved. Thus, the development of the instability driven by runaway electrons leads to the saturation of the plasma current due to the retardation effect of the runaway current fraction. Thus, the continuous creation model for the calculations of runaway current values is no more valid (Fig. 2.5).

One more deteriorative effect of the runaway instability on the discharge performance was observed in experiments. The instability itself has led to the appearance of minor disruption events even at significantly lower plasma current values, at which the threshold of distortion of the MHD equilibrium and stability could not be achieved.

2.4.3. Plasma confinement and stability modifications produced by the external generation of an edge helical current established between the two tokamak localised limiters.

Helical superficial currents of about –5A (+4 A), flowing between two diametrically opposed (vertical up and horizontal external) limiters, have been generated applying voltages of +200 V (-200 V). These currents follow two paths which, for q=2, have lengths of about one half and one and a half the vessel toroidal perimeter, respectively. Negative helical currents have originated a reduction of about 20% on the MHD spectrum amplitude and a shift of

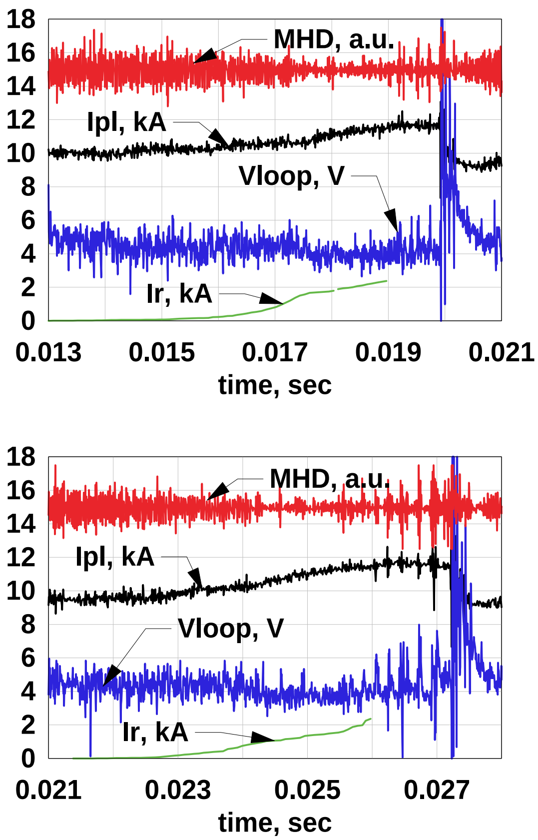

Fig. 2.5 - The evolution of plasma parameters and runaway currents between partial disruption events and during the instability driven by runaway electrons in shot #8570.
The continuous creation model for the runaway current calculation is not valid after the development of the runaway instability (i.e. after 0.019 and 0.026 secs).

the highest amplitude spectral lines to the lower frequencies. On the contrary, positive currents have led to a smaller decrease in the spectral amplitudes with a null or a very slight shift to the higher frequencies. Plasma stability has been improved by externally generated hellical surface currents. Selective interaction between these helical currents, which may follow B-lines with q values from 2 to 6 and some tearing modes with m=3 to m=6, revealed by amplitude and frequency variations of the respective spectral peaks (f<60 kHz), has been observed in some discharges.

2.4.4. Alternating limiter biasing experiments on ISTTOK and study of the associated modifications in both plasma confinement and stability

Studies similar to those made in 1998 concerning the enhancement (reduction) of the plasma confinement and stability by negative (positive) limiter biasing were performed with an alternating biasing voltage (50 Hz, 60 - 200 V p.p.). The aim of these studies was not only to confirm, in a single shot, the formerly reported transient results, obtained on several discharges with a fixed DC bias, but also to determine biasing thresholds for stability and confinement modifications and their dependence on the plasma parameters and on the growth rate of the potential applied to both limiters.

Fig. 2.6 shows that during the positive (negative) bias half-cycle we have observed: (i) a decrease (increase) of the plasma current; (ii) a large increase (small decrease) of the electron density; (iii) an increment (decrement) of the intensity of the H_α radiation; and (iv) a fall (rise) of the electron temperature.

The ratio n_e/H^{α} takes lower (higher) values during the positive (negative) bias half-period, when compared with its reference value, thus proving confinement degradation (enhancement).

At the plasma edge two Langmuir probes show that during either positive or negative bias the electron saturation current increases, when compared with the reference value. The floating potential has a temporal variation similar to that of the biasing voltage.

The Heavy Ion Beam Diagnostic, using a 22 keV Xe^+ primary beam and a multiple cell array detector, shows that the plasma radial profile is narrower and peaked for positive bias and broader, flatter and with a steeper edge for negative biasing. Further positive bias has lead to a vertical shift of the plasma column.

The alternating biased discharges are now being analysed in what concerns plasma stability. Preliminary results show that positive (negative) bias seems to lead to a poor (better) stability, translated by an increase (decrease) of the MHD activity, with both an increase (decrease) of the spectral width and a slight increase (decrease) of the frequency of the dominant tearing modes.

Thresholds for confinement and stability improvement or degradation are also being determined. First results show that confinement modifications require a biasing voltage of about 40 V ($4\ kT_e(a)/e$). This means that, for example, the

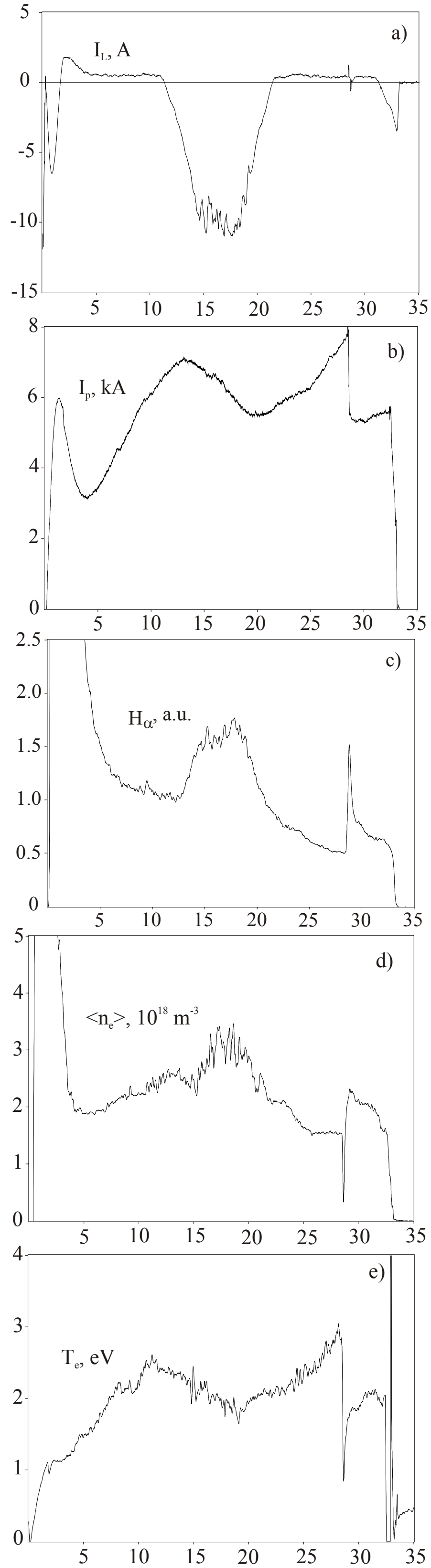

Fig. 2.6 – Evolution of the limiter (I_L) and plasma (I_p) currents, the H_α radiation, the plasma average density (<ne>) and temperature (T_e) in shot #5469. Time in ms.

beneficial effects of negative biasing are maintained during the first 2.5-3.5 ms (3-4 τ_E) in the beginning of the positive biasing half-cycle. Thresholds for other physical processes, such as modifications of the MHD activity, are also being calculated.

2.4.5. Determination of the edge plasma potential profile with the new set of emissive Langmuir probes

In fusion experiments, only cold probes have been used up to now to determine the plasma potential in the scrape-off layer (SOL), and their floating potential was assumed to be proportional to the plasma potential. However, drifting electrons or beams shift the current-voltage characteristic of a cold probe by a voltage, which corresponds to the mean kinetic energy of the drifting electrons. This problem can be avoided by the use of electron emissive probes, since an electron emission current is independent of electron drifts in the surrounding plasma. In addition emissive probes are insensitive to electron temperature fluctuations in the plasma.

An arrangement of three emissive probes was installed in the edge plasma region of ISTTOK. The probes have been mounted in such a way that the tips are positioned on the same poloidal plane but on different minor radii in the SOL. Each probe consists of a four-bore ceramic tube of 2.8 mm outer diameter. The bores have 0.5 mm diameter each. Through two of these bores, a 0.2 mm diameter W-wire has been drawn, forming a loop tip of about 5 mm in length. Inside the ceramic tube bores, each of the W-wires was spliced with about 12 copper threads of a diameter of 0.05 mm each.

The plasma potential is being measured in the edge region of ISTTOK with this arrangement of three emissive probes. The first experiments have shown that the emissive probes do not degradate the discharge quality.

2.4.6. Analysis of plasma potential changes by heavy ion beam probing with a time-of-flight method

An alternative method to that of the traditional electrostatic energy analyser for the measurement of the plasma potential has been developed based on the time-of-flight (TOF) technique.

The TOF energy analyser, built for experiments with a pulsed primary beam on ISTTOK, is shown in Fig. 2.7. The HIBD operates with 1.5 μA of a steady Cs^+ beam extracted from the plasma ion source and accelerated up to 22 keV. One pair of electrostatic plates, powered by DEI HV1000 pulser, and the following defining aperture in the primary beamline constitute the beam modulator. Beam pulses of 250 ns width are produced by fast deflection accross the aperture.

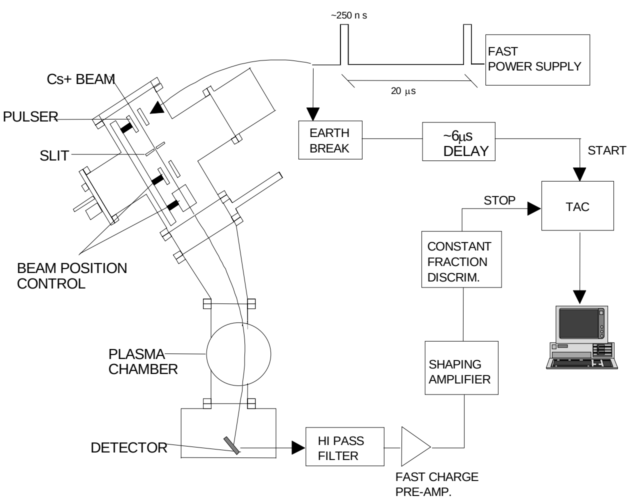

Fig. 2.7 - The one-channel time-of-flight energy analyser.

The changes of the average plasma potential during ISTTOK discharges with minor disruptions have been obtained by the HIBD with TOF energy analysis in experiments with a pulsed primary beam crossing the plasma. These measurements are based on the relation between the changes of the average plasma potential and the time-of-flight of the pulsed primary beam in two moments t and t+Δt:

$$\Delta\tau_{TOF} = \tfrac{1}{2}\tau_{TOF}(L_{pl}/L_{TOF})\int\{e\{\Phi(l_{tr}/L_{pl},t+\Delta t) - \Phi(l_{tr}/L_{pl},t)\}/E_0\}d(l_{tr}/L_{pl}) + \Delta\tau_{add} \quad (2.6)$$

where L_{pl} and L_{TOF} are respectively the length of the primary trajectory in the plasma and the full TOF path, $\Phi(l_{tr}/L_{pl},t)$ and $\Phi(l_{tr}/L_{pl},t+\Delta t)$ are the potential distributions established in moments t, t,$+\Delta t$, and the integration is performed over the primary trajectory l_{tr}. The additional term $\Delta\tau_{add}$ in the right side of Eq. 2.5 includes the effects that disturb the beam trajectory. Numerical simulations show that this term can be neglected for the parameters of the ISTTOK discharges.

The actual TOF energy analysis resolution is $\Delta\tau_{TOF}/\tau_{TOF} \sim 7.5\times10^{-4}$, and it is mainly restricted by the loading of the detector by plasma ultraviolet radiation. The relative and absolute resolutions of the measurements of the average plasma potential are estimated as $e\Delta\Phi/E_0 \cong 1.1\times10^{-2}$ and $\Delta\Phi \cong 240$ V. Temporal resolution of the measurements, determined by TAC acquisition (busy) time, is $\Delta t = 25$ µs.

Fig. 2.8 shows a typical plasma shot with the occurrence of minor disruptions. The direct analysis of the TOF signal reveals a drop of the plasma potential during disruptions although its absolute value is, for the moment, undetermined. Assuming the shortening of the radial electric field in disruptions, the plasma potential should be posistive, in opposition to the predictions of the neoclassical theory. Anomalous positive plasma potential agrees with the theoretical model for enhanced electron diffusion in a stochastic magnetic field. Thus estimated values of the plasma potential in small density discharges are considerably higher than theoretical ones, and could be the result of the presence of runaway electrons. Based on the simple model of the coaxial plasma capacitor, the estimation of the effective disbalance between the numbers of plasma electrons and ions to create the observed radial electric field is in the range of the relative population of runaways in the investigated small density discharges of ISTTOK. The observed step-by-step disappearance of the drop on the TOF signal in disruptions occurring in discharges with increasing plasma density is associated with sequential changes of the plasma potential profile with decreasing central values.

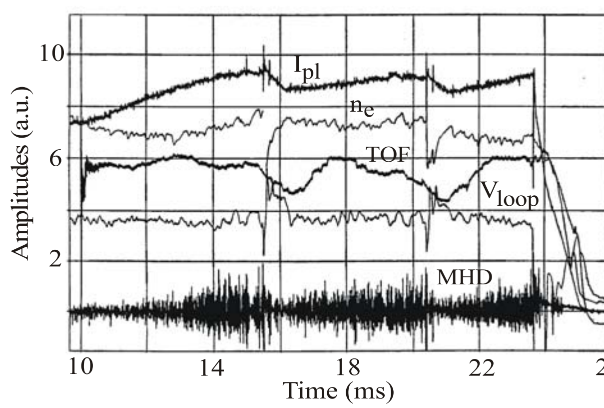

Fig.2.8 - The time evolution of the signals I_{pl}, n_e, TOF, V_{loop}, MHD in typical disruptive discharge of the tokamak ISTTOK.